

The Heliosphere—Blowing in the Interstellar Wind

Priscilla C. Frisch

University of Chicago, Chicago, IL 60637 USA

Abstract. Measurements of the velocity of interstellar He⁰ inside of the heliosphere have been conducted over the past forty years. These historical data suggest that the ecliptic longitude of the interstellar flow has increased at a rate of $\sim 0.18^\circ$ per year. Possible astronomical explanations for these short-term variations in the interstellar gas entering the heliosphere are presented.

Keywords: heliosphere, interstellar medium

PACS: 96.50.Xy

INTRODUCTION

When Leverett Davis, Jr., first proposed that the solar wind carves out a cavity in the galactic magnetic field [1], he noted that the path taken by galactic cosmic rays (GCRs) to the inner heliosphere depends on the directions between the solar and interstellar magnetic fields (ISMF). Although the angle between the ISMF direction and the vector motion of interstellar gas flowing through the heliosphere was recognized as important for determining the termination shock distance [2], the magnetically distorted heliosphere was confirmed only after Voyager 2 crossed the solar wind termination shock in 2008 [3]. Interstellar gas and dust have now been measured in the inner heliosphere by many spacecraft [4], and the direction of the local ISMF has been independently determined by the band of energetic neutral atoms (ENAs) discovered by the Interstellar Boundary Explorer (IBEX) spacecraft [5]. The modulation of galactic cosmic rays (GCRs) by the heliosphere has been known since Davis first proposed the existence of the heliosphere, but only recently have asymmetries in the GeV-TeV GCRs been directly attributed to the modulation or acceleration of GCRs in the plasma heliosphere [6, 7].

Our heliosphere is ‘blowing in the wind’ of the surrounding Local Interstellar Cloud (LIC). Like all winds, the interstellar medium (ISM) around the heliosphere changes with time over both short and long timescales, and these variations cause changes in the flux of galactic cosmic rays at 1 AU that may imprint on the radionuclide record on Earth [8].

During the forty years over which the wind of interstellar He⁰ through the heliosphere has been measured, the Sun has moved 150 AU through space, and 300 AU with respect to the LIC. Someday we might encounter one of the tiny AU-sized low column density interstellar ‘clouds’, $N(\text{H}^0) < 10^{18} - 10^{19} \text{ cm}^{-2}$, found throughout the ISM [9, 10]). The nearest of such clouds that has

been identified is in the constellation of Leo, and is ~ 20 pc away. Small scale structure of the interstellar Na⁰ line indicates spatial variations in the ISM properties over scales of 50 AU, and cold dense tiny clouds are seen as well (20 K, 3000 cm^{-3} , 200 AU [11]).

In this review, our galactic environment is briefly reviewed and evidence for short-term variations in the ISM feeding He⁰ into the heliosphere is presented, together with the implications of these variations for the local interstellar environment.

THE INTERSTELLAR MAGNETIC FIELD NEAR THE HELIOSPHERE

Convergence of the predictions for properties of the outer heliosphere boundary conditions determined from MHD heliosphere models (see other papers in this volume), and from photoionization models of the LIC [4, 12], show that the heliosphere is located in a partially ionized magnetoionic medium. The discovery in 2009 of a ‘Ribbon’ of ENAs by IBEX provided an unpredicted and unprecedented measure of the direction of the interstellar magnetic field (ISMF) that shapes the heliosphere. Comparisons between 1 keV ENA data and 3D MHD heliosphere models indicated that the Ribbon traces viewpoints where the ISMF draping over the heliosphere is perpendicular to the radial sightline [13]. The pressure of ENAs in the heliosheath indicates a strength for the ISMF shaping the heliosphere of $\sim 3 \mu\text{G}$ [14], which is comparable to the expected LIC field strength if thermal and gas pressures are comparable [12, 15].

Although details of the Ribbon formation are not yet understood, models suggest the Ribbon originates 10–100 AU upstream of the heliopause [13, 16, 17, 18]. In the models, the locus of Ribbon points moves towards the equator of the ISMF as either the field strength becomes stronger [16, 17], or the formation region moves further

from the heliopause [19].

We have undertaken a program to find the ISMF direction in the ISM near the Sun, employing measurements of the polarization of starlight that results from paths through clouds containing magnetically aligned dust grains [20]. The E-vector of the polarization is parallel to the ISMF direction in the diffuse ISM (e.g. [21]). We developed a method to determine the ISMF direction from an ensemble of measurements of the polarization position angles (e.g. the angle between the polarization direction and the north pole). We have found that the nearby, < 20 pc, ISMF is aligned with the axis through $\ell, b = 47^\circ \pm 20^\circ, 25^\circ \pm 20^\circ$ (optical polarization data do not provide the field polarity). This direction is $32^\circ \pm 30^\circ$ from the center of the Ribbon arc, located at $\ell, b = 33^\circ \pm 4^\circ, 55^\circ \pm 4^\circ$.

The ISMF traced by the polarization data appears to have an ordered component that extends to within 8 pc of the Sun. The ordered component of this very local field rotates slowly at a rate of $\sim 0.25^\circ$ per parsec. Superimposed on this field is a turbulent component of $\sim 23^\circ$ [20]. Since the Ribbon arc itself can be centered up to 16° away from the ISMF direction outside of the heliosphere according to the models [16], and the field rotates slowly, in my view we can consider the ISMF directions obtained from the polarization data to be consistent with the direction of the ISMF that shapes the heliosphere.

Figure 1 shows the direction of best-fitting ISMF direction (solid lines) against the distribution of interstellar dust within 100 pc. The large white arc-like structure shows the interstellar dust associated with Loop I, which is a giant magnetic bubble that appears to extend to the solar location (see below). The very local ISMF may be part of the Loop I magnetic field (see below).

HELIOSPHERE AND ENVIRONMENT

The relative Sun-interstellar velocity drives interstellar gas and larger dust grains into the inner heliosphere, while the interstellar magnetic field, ionized gas, and tiny charged grains are deflected around the heliopause. As is well known, neutral interstellar gas is ionized in the heliosphere by charge-exchange (CEX) with solar wind plasma, photoionization, and/or electron impact ionization, depending on the species. Charge exchange between the solar wind and interstellar H^0 creates ENAs that are mapped by IBEX, revealing the time-variable heliosphere plasmas. Ionized interstellar atoms are convected outwards with the solar wind as a population of evolving pickup ions (PUI) that seed the formation of anomalous cosmic rays (ACR). All of the abundant atoms that have significant neutral fractions in the interstellar cloud around the heliosphere, e.g. H, He, N,

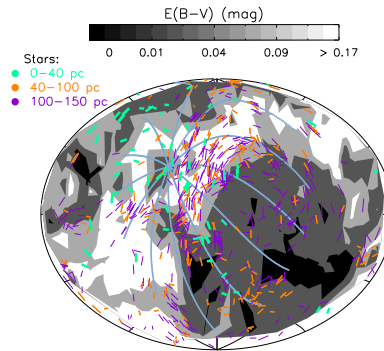


FIGURE 1. Directions of optical polarizations are shown projected against the distribution of interstellar dust within 100 pc, as traced by color excess $E(B-V)$ measurements. The polarizations trace the ISMF direction. The lines show the best-fitting local ISMF direction from starlight polarized in the ISM. The white arc-like region shows the distribution of interstellar dust that traces the boundary regions of Loop I within 100 pc. The dark regions in the third and fourth galactic quadrants correspond to the deficit of local ISM associated with the Local Bubble, which also corresponds to the regions with the brightest local UV and EUV radiation fluxes because of low interstellar opacities. The data are plotted in an airtoff projection, centered on the galactic center and with longitude increasing to the left. See [20] for more details

O, Ne, and Ar, have been either directly detected or observed in the form of PUIs or ACRs [4]. When combined, these data show that the LIC is a warm, low density, partially ionized interstellar cloud, with the isotopic composition of the Sun, and that arrives at the Sun from a direction within 15° of the galactic center [22, 4].

Reasonable values for the parameters of the LIC at the heliosphere boundaries have been reviewed in Frisch et al. [4]. Densities of H^0 , protons, and He^0 are, respectively, 0.19 cm^{-3} , 0.07 cm^{-3} , and $0.015 \pm 0.003 \text{ cm}^{-3}$. The He^0 density is based on Ulysses measurements near 5 AU where particle trajectories have not yet been distorted by solar gravity into the downwind focusing cone [23]. Measurements of interstellar He^0 at 1 AU by IBEX-LO show that ISM flows through the heliosphere at a velocity of $23.2 \pm 0.3 \text{ km s}^{-1}$ and a temperature of $6300 \pm 390 \text{ K}$, with the flow directed towards galactic coordinates of $\ell, b = 185.25^\circ \pm 0.24^\circ, -12.03^\circ \pm 0.51^\circ$ (see Table 1 for ecliptic coordinates [24]).

The penetration depth of neutral interstellar atoms into the heliosphere differs between elements, depending mainly on the CEX cross-section. Helium and neon are on hyperbolic trajectories, becoming ionized within 1 AU of the Sun, and form density enhancements downwind of the Sun that are known as 'focusing tails' [23, 25]. In contrast, the density distribution of neutral interstellar hydrogen is strongly modified by CEX in the

inner and outer heliosheath regions and inner and outer heliosheath regions and the heliosphere, and by radiation pressure closer to the Sun. The complex H⁰ source function, with contributions from primary and secondary particle populations [26], temporal variations in the solar L α flux that affect trajectories and backscattered emission [27], and $\sim 50\%$ filtration, challenges efforts to extract an accurate LIC velocity vector from the H⁰ backscattered data. Thus the most reliable measure of the LIC velocity is obtained from data on interstellar He⁰ inside of the heliosphere.

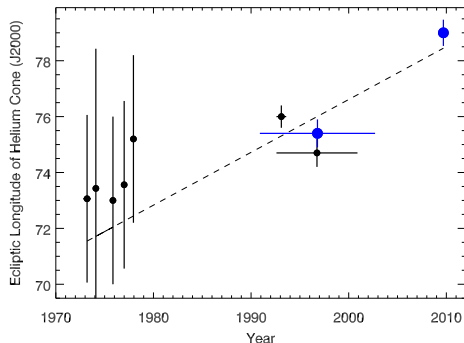


FIGURE 2. Directions of the flow of interstellar He⁰ from direct detection of He atoms (after 1990), and the fluorescence of the EUV 584Å line (20th century, see Table 1). Although the earlier results have been discounted [28] since they did not agree with the results of the Ulysses GAS detector [29, 23], the most recent precise measurement by IBEX [24] indicate that there may be a real temporal variation in the direction of the ISM flowing into the heliosphere. If so, the results plotted in this figure suggest that the ecliptic longitude of the wind direction varies at approximately $\delta\lambda \sim 0.18^\circ$ per year. The width of the horizontal bars for each point show the earliest and latest times over which the data were collected. The large blue points are the IBEX and Ulysses *in situ* values.

BLOWING IN THE WIND

Historical helium data

The velocity vector of the flow of interstellar He⁰ through the heliosphere has been determined many times over the past 40 years. The directions of the He⁰ flow have been either determined from the weak resonant scattering of solar 584Å emission by interstellar He⁰ in the heliosphere, or from *in situ* He⁰ measurements. The historical variations of the He⁰ flow direction is plotted in Figure 2. The blue points in Figure 2 represent directions determined from *in situ* measurements of He⁰ by Ulysses [29] and IBEX [24]. The He⁰ velocity, beginning and end times of the measurements, and downwind ecliptic

longitude of the velocity are listed in Table 1, where most directions have been precessed to J2000 coordinates.

Interstellar helium enters the heliosphere with minimal filtration, and trajectories are determined by the position, velocity, and temperature of the particles, solar gravity, and ionization due to photoionization and electron impact ionization within 1 AU [30]. The details of the models used to obtain the He⁰ vectors vary between the different sets of data, particularly for the older data where the models are less developed and solar flux data were not reliable.

These data provide a basis for evaluating temporal variations in the interstellar boundary conditions of the heliosphere. Figure 2 shows that the ecliptic longitude of the He⁰ velocity vector has steadily increased with time over the past forty years (Table 1). A linear fit to the data suggests an increase of $\sim 0.18^\circ$ per year in the ecliptic longitude of the He flow. Over the same interval the ISMF rotation would be only 1/100th of an arcminute based on the polarization data. At this rate, the direction of the LIC flow would change by 90° over 500 years. Depending on the behavior of the ISMF, the heliosphere configuration should also vary dramatically over timescales of several centuries..

Assuming that the time-dependence of the He⁰ direction is real, I will now look at possible interstellar explanations for this variation.

Why the change?

It has been argued that the older data are inaccurate because of instrumental uncertainties or poorly known ionization corrections. In an effort to make the older Prognos 6 He⁰ data [35] consistent with the Ulysses GAS results [29], Lallement et al. [28] found that the two sets of results could be brought into agreement if the instrumental noise was decoupled from the pre-launch laboratory calibration and added as a variable into the analysis. However this type of argument can not explain the even steeper temporal variation between the wind longitudes found by IBEX versus Ulysses (Figure 2).

One might speculate that the slow increase in ecliptic longitude of the velocity is due to variations in solar conditions over the past 40 years. At a given spatial position, the He⁰ atom may have arrived directly from the ISM, or may have arrived indirectly through close passage by the Sun on the downwind side due to gravitational focusing [39]. An apparent shift in the direction could occur if there were a systematic variation in the mix of direct and indirect atoms that are detected, perhaps due to variations in the ionization rates of the indirect atoms traveling close to the Sun where losses from electron impact ionization and photoionization dominate. Such an explanation would not explain the difference between Ulysses

TABLE 1. Interstellar gas velocity obtained from interstellar He^o data

Start/End of data*	Velocity (km s ⁻¹)	Downwind λ, β	Coord. epoch [†]	Ref.
1972.8/1973.6	5–20	73.1 ± 3, -8.34 ± 3	2000	Weller & Meyer [31]
1974.1/1974.1	[22 ± 3]**	73.4 ± 5, -5.4 ± 5	2000	Ajello et al. [32]
1975.6/1976.1	9–27	73. ± 3, -7.34 ± 3	2000	Weller & Meier [33]
1976.9/1977.1	22–28	73.6 ± 3, -4.37 ± 3	2000	Weller & Meier [34]
1977.8/1978.1	27 ± 3	75.2 ± 3, -6 ± 3 xxx	2000	Daladier et al. [35]
1990.9/2002.7	26.3 ± 0.4	75.4 ± 0.5, -5.1 ± 0.2	2000	Witte [29]
1992.6/1993.6	26.4 ± 1.5	76.0 ± 0.4, -5.4 ± 0.6		Flynn et al. [36]
1992.6/2000.9	24.5 ± 2.0	74.7 ± 0.5, -5.7 ± 0.5		Vallerga et al. [37]
2009.2/2010.2	23.2 ± 0.4	79.00 ± 0.47, -4.98 ± 0.21	2000	McComas et al. [24]

* Column 1 shows the first and last year of data acquisition.

[†] J2000 coordinates were either obtained by precessing B1950 celestial coordinates, or originally provided as J2000 coordinates. Other values were taken directly from the references.

** The *Copernicus* velocity was assumed from Adams & Frisch [38].

and IBEX values, since some Ulysses data were acquired near 5 AU before the flow characteristics become distorted by solar gravity. Sunspot activity levels vary between the different sets of measurements, but no systematic trend is associated with the data listed in the Table.

A more interesting possibility, that I prefer, is that the direction of the ISM flow through the heliosphere is time-dependent.

Cloud edges

Cloud edges are interesting properties of the ISM that are difficult to study, and the Sun is near a cloud edge. It is now well known that an absorption component at the LIC velocity has not been seen towards stars in the upwind direction. The most compelling example is 36 Oph, which is a star 6 pc away and 9° from the heliosphere nose direction. Towards this star, the velocities of the interstellar Fe⁺, Mg⁺, and D^o lines are 28.3 ± 0.5 km s⁻¹ [40] in contrast to the ~ 23.2 km s⁻¹ that is predicted from the He^o LIC velocity. This indicates that for an average LIC density of 0.19 cm⁻³, the Sun is less than 20,000 AU (0.1 pc) from the LIC boundary.

The properties of the LIC cloud edge depend on the interaction of the LIC and the adjacent ISM. Within 10 pc, only 25%–40% of space is filled with observable ISM. The LIC is part of a flow of ISM (the cluster of local interstellar clouds, CLIC) with an upwind direction directed towards the center of the Loop I evolved superbubble, more specifically the S1 shell part of Loop I and the flow is decelerating ([4, 41], and see below). A possibility for the edge region of the LIC in the upwind direction is that it is influenced by cloud collisions, since the flow of nearby ISM is not a rigid body but rather is compressed towards the Sun from both the extreme upwind and extreme downwind directions [42, 43]. For example,

Schwadron et al. [6] explain the GCR asymmetries related to the heliosphere in terms of a magnetic field disturbance caused by the collision of the LIC and another cloud in the downwind direction. A second possibility is that the LIC is embedded in the hot plasma of the Local Bubble, and a hot conductive interface or turbulent mixing layer is present at the LIC edge.

The one piece of information that we have is that the change in the flow direction is such that the flow is moving away from the direction of the ISMF that shapes the heliosphere, which is towards $\lambda, \beta = 221^\circ, 39^\circ$ according to the center of the IBEX Ribbon arc [5, 44]. Note that the latitude variations are smaller and less well constrained than the longitude variations. This would seem to indicate that the ISM feeding the He^o into the heliosphere has become less ionized over time, since increased ionization would couple the flow more tightly to the ISMF. The decreasing-ionization scenario is consistent with a local gradient in the interstellar radiation field that is defined by the lower opacity and higher radiation fluxes found in the galactic interval $\ell \sim 190^\circ - 360^\circ$ (Figure 1, [20]).

Turbulence

Based on the trend for the ecliptic longitude of the LIC velocity vector to increase with time, it should be considered a real possibility that the Sun has sampled turbulence in the LIC velocity over the past several decades.

The average values for the temperature and turbulence of the LIC are 7,500 ± 1,300 K and 1.62 ± 0.75 km s⁻¹, based on absorption lines toward 19 stars behind the LIC according to Redfield et al. [45]. Nonthermal turbulence is calculated by assuming that the full-width-half-max of the absorption line is proportional to $(V_{\text{thermal}}^2 + V_{\text{turbulence}}^2)^{1/2}$, where V_{thermal} is the Doppler

spread in thermal velocities appropriate for the cloud temperature, and $V_{\text{turbulence}}$ represents non-thermal contributions to the velocity over the length of the sightline. Uncertainties in this type of analysis can incorporate gradients in the velocity field, or even blended absorption components, into the turbulence parameter depending on spectral resolution and data quality (e.g. [46]).

If the average line width of the LIC is attributed to the ISM entering the heliosphere, but with a temperature $\sim 6,300$ K as found from the He^o data, then the turbulent velocity would be 4.7 km s^{-1} . There is no information about the scale size of the turbulence in the LIC, so according to these arguments, a plausible case can be made that this nominal 4.6 km s^{-1} turbulent component samples turbulence in the ISM between the Sun and the upwind edge of the LIC. In such a case, a systematic variation in the flow direction is possible.

Filaments in the magnetoionized medium

A gradient in the magnetic field strength between the heliosphere and the edge of the LIC is also possible. Turbulence in the galactic magnetic field manifests itself in the magnetoionic ISM over large spatial scales through structures that appear in maps of the polarized radio continuum, but which are not visible in the radio continuum intensity maps. Gaensler et al. [47]. have shown that these structures form a web of filaments that do not appear to be supersonic. Most interesting for the local ISM is that the spatial gradient of the radio continuum polarization is such that the polarization changes more rapidly for directions that are perpendicular to the filamentary elongations. If the LIC is elongated along the ISMF direction as given by the IBEX Ribbon, the gradient in the ISMF would make an angle of $\sim 42^\circ$ with respect to the He^o flow vector. The gradient in the ISMF would influence the heliosphere and secondary He^o feature discovered by IBEX [48], and possibly the mix of primary and indirect He^o atoms that are detected.

Loop I superbubble

My last possible explanation for the variable ISM direction inside of the heliosphere is a hand-waving argument, based on the dynamic structure of the ISM near the Sun, which seems to be related to the Loop I superbubble. Three epochs of star formation in the nearby Sco-Cen Association formed Loop I (e.g.[4]). Comparisons between optical and synchrotron polarization data show that the ISMF is parallel to the elongated filaments that form the observed structure of Loop I (e.g. [49]). The brightest part of Loop I in the 1.8 MHz radio continuum is a region known as the North Polar Spur, where the den-

sity of the ISM increases continuously from the Sun out to ~ 100 pc [50, 51, 20]. The local ordered ISMF discussed above is directed towards the North Polar Spur.

Three sets of data suggest that the Sun is near or in a fragment of the shell of the Loop I superbubble: (1) The Loop I model of Wolleben [52, 53] identifies two radio continuum shells (called “S1” and “S2”) at different distances and locations. The Sun is located in the rim of the S1 shell according to his model, a result that agrees with prior estimates of the Loop I configuration [54]. (2) Interstellar clouds within about 20 pc of the Sun, e.g. the CLIC, have a bulk velocity in the local standard of rest (LSR, e.g. after solar motion with respect to nearby cool stars is subtracted) that is within 15° of the center of the S1 shell, suggesting an expanding shell configuration [53, 4]. (3) The local ISMF directions found from the center of the IBEX Ribbon arc, and from the interstellar polarization measurements, both have angles $\sim 76^\circ$ away from the bulk local ISM flow, and $\sim 64^\circ$ from the S1 center as defined by Wolleben.

In conclusion, there are many astronomical justifications for the hypothesis that the very local ISM varies over spatial scales that are comparable to the heliosphere size. After all, the heliosphere itself provides a major disruption of the ISM and ISMF over spatial scales of $> 10,000$ AU, or equivalently 0.05 pc. A reanalysis of the historical He^o data is needed to check my basic conclusion that the direction of the flow of interstellar gas through the heliosphere has varied over the space age.

ACKNOWLEDGMENTS

This work has been supported by the IBEX mission as part of the NASA Explorer Program.

REFERENCES

1. L. Davis, *Physical Review* **100**, 1440–1444 (1955).
2. T. E. Holzer, *ARA&A* **27**, 199–234 (1989).
3. E. C. Stone, A. C. Cummings, F. B. McDonald, B. C. Heikkila, N. Lal, and W. R. Webber, *Nature* **454**, 71–74 (2008).
4. P. C. Frisch, S. Redfield, and J. Slavin, *ARA&A* **49** (2011).
5. D. J. McComas, F. Allegrini, P. Bochsler, Christian, G. B. Crew, R. DeMajistre, H. Fahr, H. Fichtner, P. C. Frisch, H. O. Funsten, S. A. Fuselier, G. Gloeckler, M. Gruntman, J. Heerikhuisen, V. Izmodenov, P. Janzen, P. Knappenberger, S. Krimigis, H. Kucharek, M. Lee, G. Livadiotis, S. Livi, R. J. MacDowall, D. Mitchell, E. Möbius, T. Moore, N. V. Pogorelov, D. Reisenfeld, E. Roelof, L. Saul, N. A. Schwadron, P. W. Valek, R. Vanderspek, P. Wurz, and G. P. Zank, *Science* **326**, 959– (2009).
6. N. A. Schwadron, F. C. Adams, B. Dingus, H. Funsten, P. Desiati, P. Frisch, and D. J. McComas, title = "

- Anisotropies in TeV Cosmic Rays Related to Entry into the Heliosphere and the IBEX Ribbon", *submitted to ApJ* **00**, 00 (2012).
7. A. Lazarian, and P. Desiati, *ApJ* **722**, 188–196 (2010).
 8. P. C. Frisch, and H.-R. Mueller, *Space Sci. Rev.* pp. 130–+ (2011).
 9. C. Heiles, *ApJ* **481**, 193–204 (1997).
 10. D. R. Saul, J. E. G. Peek, J. Grcevich, M. E. Putman, K. A. Douglas, E. J. Korpela, S. Stanimirović, C. Heiles, S. J. Gibson, M. Lee, A. Begum, A. R. H. Brown, B. Burkhart, E. T. Hamden, N. M. Pingel, and S. Tonnesen, *ApJ* **758**, 44 (2012).
 11. D. M. Meyer, J. T. Lauroesch, J. E. G. Peek, and C. Heiles, *ApJ* **752**, 119 (2012).
 12. J. D. Slavin, and P. C. Frisch, *A&A* **491**, 53–68 (2008).
 13. N. A. Schwadron, M. Bzowski, G. B. Crew, *Science* **326**, 966– (2009).
 14. N. A. Schwadron, F. Allegrini, M. Bzowski, E. R. Christian, G. B. Crew, M. Dayeh, R. DeMajistre, P. Frisch, H. O. Funsten, S. A. Fuselier, K. Goodrich, M. Gruntman, P. Janzen, H. Kucharek, G. Livadiotis, D. J. McComas, E. Moebius, C. Prested, D. Reisenfeld, M. Reno, E. Roelof, J. Siegel, and R. Vanderspek, *ApJ* **731**, 56–77 (2011).
 15. P. C. Frisch, "How local is the local interstellar magnetic field?," in *Am. Inst. Phys. Conf. Ser.*, edited by J. Heerikhuisen, G. Li, N. Pogorelov, and G. Zank, 2012, vol. 1436 of *Am. Inst. Phys. Conf. Ser.*, pp. 295–301.
 16. J. Heerikhuisen, and N. V. Pogorelov, *ApJ* **738**, 29–+ (2011).
 17. R. Ratkiewicz, M. Strumik, and J. Grygorczuk, *ApJ* **756**, 3 (2012).
 18. S. V. Chalov, D. B. Alexashov, D. McComas, V. V. Izmodenov, Y. G. Malama, and N. Schwadron, *ApJ* **716**, L99–L102 (2010).
 19. P. C. Frisch, and D. J. McComas, *Space Sci. Rev.* (2010), [ArXiv/astroph-G:1012.0586](https://arxiv.org/abs/1012.0586).
 20. P. C. Frisch, B. Andersson, A. Berdyugin, H. O. Funsten, M. Magalhaes, D. J. McComas, W. DeMajistre, V. Piirola, N. A. Schwadron, J. D. Slavin, and S. J. Wiktorowicz, *ApJ*, in press p. 00 (2012).
 21. B.-G. Andersson, *ArXiv e-prints/astro-ph:1208.4393* (2012), [1208.4393](https://arxiv.org/abs/1208.4393).
 22. P. C. Frisch, M. Bzowski, E. Grün, V. Izmodenov, H. Krüger, J. L. Linsky, D. J. McComas, E. Möbius, S. Redfield, N. Schwadron, R. R. Shelton, J. D. Slavin, and B. E. Wood, *Space Sci. Rev.* **146**, 235–273 (2009).
 23. E. Möbius, M. Bzowski, S. Chalov, H. Fahr, G. Gloeckler, V. Izmodenov, R. Kallenbach, R. Lallement, D. McMullin, H. Noda, M. Oka, A. Pauluhn, J. Raymond, D. Ruciński, R. Skoug, T. Terasawa, W. Thompson, J. Vallergera, R. von Steiger, and M. Witte, *A&A* **426**, 897–907 (2004).
 24. D. J. McComas, D. Alexashov, M. Bzowski, H. Fahr, J. Heerikhuisen, V. Izmodenov, M. A. Lee, E. Möbius, N. Pogorelov, N. A. Schwadron, and G. P. Zank, *Science* **336**, 1291– (2012).
 25. P. Bochsler, L. Petersen, E. Möbius, N. A. Schwadron, P. Wurz, J. A. Scheer, S. A. Fuselier, D. J. McComas, M. Bzowski, and P. C. Frisch, *ApJS* **198**, 13 (2012).
 26. E. Quémerais, and V. Izmodenov, *A&A* **396**, 269–281 (2002).
 27. E. Quémerais, Y. G. Malama, W. R. Sandel, R. Lallement, J. . Bertaux, and V. B. Baranov, *A&A* **308**, 279–289 (1996).
 28. R. Lallement, J. C. Raymond, J. Vallergera, M. Lemoine, F. Dalaudier, and J. L. Bertaux, *A&A* **426**, 875–884 (2004).
 29. M. Witte, *A&A* **426**, 835–844 (2004).
 30. M. Bzowski, M. A. Kubiak, E. Möbius, P. Bochsler, T. Leonard, D. Heirtzler, H. Kucharek, J. M. Sokół, M. Hłond, G. B. Crew, N. A. Schwadron, S. A. Fuselier, and D. J. McComas, *ApJS* **198**, 12 (2012).
 31. C. S. Weller, and R. R. Meier, *ApJ* **193**, 471–476 (1974).
 32. J. M. Ajello, N. Witt, and P. W. Blum, *A&A* **73**, 260–271 (1979).
 33. C. S. Weller, and R. R. Meier, *ApJ* **227**, 816–823 (1979).
 34. C. S. Weller, and R. R. Meier, *ApJ* **246**, 386–393 (1981).
 35. F. Dalaudier, J. L. Bertaux, V. G. Kurt, and E. N. Mironova, *A&A* **134**, 171–184 (1984).
 36. B. Flynn, J. Vallergera, F. Dalaudier, and G. R. Gladstone, *J. Geophys. Res.* **103**, 6483 (1998).
 37. J. Vallergera, R. Lallement, M. Lemoine, F. Dalaudier, and D. McMullin, *A&A* **426**, 855–865 (2004).
 38. T. F. Adams, and P. C. Frisch, *ApJ* **212**, 300–308 (1977).
 39. H.-R. Müller, and J. H. Cohen, "Primary neutral helium in the heliosphere," in *Am. Inst. Phys. Conf. Ser.*, edited by J. Heerikhuisen, G. Li, N. Pogorelov, and G. Zank, 2012, vol. 1436 of *Am. Inst. Phys. Conf. Ser.*, pp. 233–238.
 40. B. E. Wood, J. L. Linsky, and G. P. Zank, *ApJ* **537**, 304–311 (2000).
 41. P. C. Frisch, L. Grodnicki, and D. E. Welty, *ApJ* **574**, 834–846 (2002).
 42. P. C. Frisch, L. Grodnicki, and D. E. Welty, *ApJ* **574**, 834–846 (2002).
 43. J. L. Linsky, B. J. Rickett, and S. Redfield, *ApJ* **675**, 413–419 (2008), [arXiv:0711.1144](https://arxiv.org/abs/0711.1144).
 44. H. O. Funsten, F. Allegrini, G. B. Crew, R. DeMajistre, P. C. Frisch, S. A. Fuselier, M. Gruntman, P. Janzen, D. J. McComas, E. Möbius, B. Randol, D. B. Reisenfeld, E. C. Roelof, and N. A. Schwadron, *Science* **326**, 964–967 (2009).
 45. S. Redfield, and J. L. Linsky, *ApJ* **673**, 283–314 (2008).
 46. D. E. Welty, and L. M. Hobbs, *ApJS* **133**, 345–393 (2001).
 47. B. M. Gaensler, M. Haverkorn, B. Burkhart, K. J. Newton-McGee, R. D. Ekers, A. Lazarian, N. M. McClure-Griffiths, T. Robishaw, J. M. Dickey, and A. J. Green, *Nature* **478**, 214–217 (2011).
 48. E. Möbius, P. Bochsler, M. Bzowski, D. Heirtzler, M. A. Kubiak, H. Kucharek, M. A. Lee, T. Leonard, N. A. Schwadron, X. Wu, S. A. Fuselier, G. Crew, D. J. McComas, L. Petersen, L. Saul, D. Valovcin, R. Vanderspek, and P. Wurz, *ApJS* **198**, 11 (2012).
 49. C. Heiles, "The Magnetic Field Near the Local Bubble," in *IAU Colloq. 166: The Local Bubble and Beyond*, edited by D. Breitschwerdt, M. J. Freyberg, and J. Truemper, 1998, vol. 506 of *Lecture Notes in Physics, Berlin Springer Verlag*, pp. 229–238.
 50. F. P. Santos, W. Corradi, and W. Reis, *ApJ* **728**, 104–+ (2011).
 51. J. Bailey, P. W. Lucas, and J. H. Hough, *MNRAS* pp. 586–+ (2010).
 52. M. Wolleben, *ApJ* **664**, 349–356 (2007).
 53. P. C. Frisch, *ApJ* **714**, 1679–1688 (2010).
 54. P. C. Frisch, *Space Sci. Rev.* **78**, 213–222 (1996).